International Journal of Impact Engineering 35 (2008) 1427–1434

Contents lists available at ScienceDirect

International Journal of Impact Engineering

journal homepage: www.elsevier.com/locate/ijimpeng

Application of Wavelet Transform to analyze acceleration signals generated by HVI on thin aluminum plates and all-aluminum honeycomb sandwich panels

A. Bettella*, A. Francesconi, D. Pavarin, C. Giacomuzzo, F. Angrilli

CISAS "G. Colombo", University of Padova, via Venezia 15, 35131 Padova, Italy

ARTICLE INFO

Article history:
Received 7 May 2007
Accepted 6 June 2008
Available online 25 July 2008

Keywords:
Wavelet analysis
Hypervelocity impacts
Shock response spectra
Wave propagation

ABSTRACT

Among all possible dangers, hypervelocity impacts on structures produce also a disturbance field, which results from the superimposition of vibrations originating on the impact point and then reflected at the target boundaries. Such disturbance environment is composed by waves of different amplitudes, frequency contents, speeds and directions of propagation. The aim of this paper is to characterize this complex environment, through the identification of its fundamental constituents using the Wavelet Transform analysis method, useful for studying transient phenomena, including wave propagation. Common signal analysis tools, like Shock Response Spectrum (SRS), cannot provide a good description of the physical behavior of such waves, nor they can differentiate between them since their frequency decomposition does not retain any time information. On the contrary, Wavelets associate a time information to the frequency content: each wave can be characterized by its frequency band and arrival time. Starting from both numerical and experimental acceleration data from impacts on aluminum plates and aluminum honeycomb sandwich panels, Wavelet analysis was employed to identify symmetric and antisymmetric waves. Moreover, reflections and dispersion phenomena were observed, leading to wave distortion due to different speeds of propagation of wave trains characterized by different frequency contents.

1. Introduction

Hypervelocity impacts (HVIs) are common problems in the space environment. Impact phenomena of space debris and micrometeoroids concern space missions, in terms of potential damage to spacecraft and satellites. Shock generation and propagation of transient vibrations represent a secondary effect of impacts and the HVI-induced vibrations field can cause malfunctioning or breaking of sensible electronic components and sensors [1]. An extensive experimental campaign was carried out at the CISAS Light Gas Gun (LGG) facility in the framework of the ESA contract "Spacecraft Disturbances from HVI", with the aim of characterizing the HVI-induced vibration field. The perturbations generated on test targets representative of real satellite structures (aluminum and CFRP honeycomb panels) were assessed through acceleration measurements, which were presented and analyzed in the form of Shock Response Spectra (SRS).

SRS is the standard shock signal analysis tool and is used to provide information about the threat level of the acceleration on nearby components. SRS is numerically computed applying the acceleration time history as base excitation to a simplified model of the component, which is represented as a certain number of one-degree-of-freedom systems (1 dof). The SRS is defined as the magnitude of the peak response at a frequency corresponding to the resonance of each individual system. SRS is a useful design tool for evaluating loads transferred by a transient-loaded structure to a sensitive object mounted on it, which must withstand the high frequency/amplitude transient acceleration. However, SRS has some drawbacks related to the overall information it provides, which cannot go into detail of the source of the threat (such as wave generating, propagating and reflecting after an impact).

Therefore, the objective of this paper is to discuss a possible method to characterize the complex vibration field generated by HVI using the Wavelet Transform (WT). Wavelets can be used in the analysis of transient signals and have the ability of identifying the different types of waves which form a complex signal, highlighting their morphology, speed of propagation and frequency content. [3,5,6] Moreover, Wavelet analysis allows studying wave's superimposition, interference and reflections in correspondence of structural edges and discontinuities.

The remainder of the paper is organized as follows. Section 2 briefly reviews the analytic equations describing the propagation of elastic waves inside plates. These will be further used to introduce the dispersion characteristic, fundamental to understand the WT

* Corresponding author. Tel.: +39 049 807 95 23; fax: +39 049 827 68 55.
E-mail address: alberto.bettella@unipd.it (A. Bettella).

0734-743X/$ – see front matter © 2008 Elsevier Ltd. All rights reserved.
doi:10.1016/j.ijimpeng.2008.07.013

method applied to signals obtained from numerical simulations and experiments. Section 3 deals with WT validation performed applying this method to acceleration time histories obtained from impact tests on simple aluminum plates. Signals were retrieved from SPH simulations and experimental data, in case of low-velocity impacts. Section 4 presents the Wavelet analysis performed on acceleration signal recorded form HVI on simple aluminum plates, while Section 5 describes the Wavelet analysis performed on acceleration signals recorded from HVI on honeycomb sandwich panels, providing a description of the complex perturbations environment on both these type of targets. Finally, conclusions are given in Section 6.

2. Mathematical model of elastic waves inside plates

Analytical solutions are presented hereafter for the propagation of elastic waves inside plates [2]. Starting from the 3D equations of waves, solutions are searched for to represent harmonic perturbations; this leads to an algebraic relation (frequency equation) whose roots describe different wave shapes: each of them is characterized by a particular frequency and speed of propagation. This decomposition is useful since any complex disturbance can be obtained by an appropriate superimposition of such elementary harmonic wave constituents. In particular, elastic perturbations generated by an impact have a narrow width in time (because of the short duration of the phenomenon) and therefore they can be thought as the sum of waves spread in a large frequency band (wider bands result form shorter waves); this set of waves is called wave group. The remainder of this paragraph presents the 3D equation of waves and the harmonic form for its solution [2]. After that, the solution of the frequency equation is discussed to show the theoretical dependence which exists between the shape of harmonic waves, their speed of propagation and frequency content. The reference model is an unconstrained homogeneous flat aluminum plate [2]. The plate and reference axes are shown in Fig. 1.

Eq. (1) is the 3D (exact) wave equation for an elastic body:

$$(\lambda+\mu)\nabla\Delta+\mu\nabla^2 u = \rho\frac{\partial^2 u}{\partial t^2} \tag{1}$$

where $u = u(x,y,z,t)$ is the vector displacement, λ and μ are the material Lamé constants and $\Delta = \nabla u = \varepsilon_x+\varepsilon_y+\varepsilon_z$ is the dilatation of the material in the three axes directions. Eq. (2) below represents a 3D harmonic wave, which is the elementary constituent of real waves.

$$\begin{aligned} u_x(x,y,z,t) &= h(y)e^{i(\xi x-\omega t)} \\ &\quad\times u_y(x,y,z,t) \\ &= i(y)e^{i(\xi x-\omega t)} \\ &\quad\times u_z(x,y,z,t) = j(y)e^{i(\xi x-\omega t)} \end{aligned} \tag{2}$$

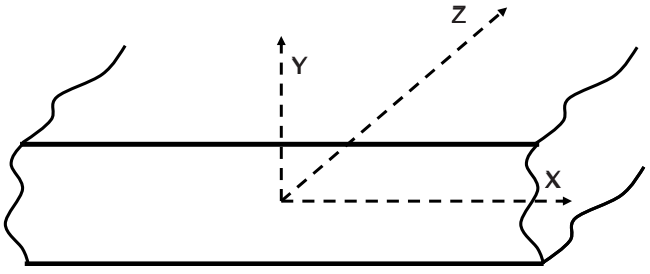

Fig. 1. Reference axis for the plate used in the mathematical model. The plate has infinite extent in the x and z directions.

where ω is the radial frequency and ξ is the wavenumber (the ratio between ω and ξ equals the wave phase speed $\omega/\xi = c$). $h(y)$, $i(y)$ and $j(y)$ are the amplitudes of the three displacements, which vary along the plate thickness.

The waves described by Eq. (2) travel along the plate length (x direction) and change their amplitude along the plate's thickness (y direction). The values for ω, ξ and for the amplitude function are calculated through the substitution of Eq. (2) into Eq. (1) and adding the boundary conditions (the plate surfaces are traction free; see Ref. [2] for the complete development of the equations). The wave solutions, Eq. (2), are shown in Fig. 2.

In Fig. 2, Ω is the dimensionless wavenumber, c is the dimensionless phase velocity and d is half of the plate thickness. Each curve represents a solution of Eq. (2) and the corresponding allowed values ξ and ω. For example, an S_0 wave can propagate in an infinite plate only if its radial frequency ω and wavenumber ξ belong to the S_0 curve shown in Fig. 2. Fig. 3 shows the resulting displacement modes, if the A_0 and S_0 solutions are taken. It is worth highlighting that the solutions (Eq. (2)) can be divided in two components: symmetric and antisymmetric with respect to the plate mid plane. Symmetric (S) and antisymmetric (A) waves (also called Lamb or guided waves) can propagate with various displacement modes, represented with increasing indexes (A_0, A_1, A_2, S_0, S_1, higher index characterize a more complex displacement pattern).

Each wave displacement mode is the result of the interference of waves traveling inside the material and bouncing at the plate surfaces. These bouncing waves can be dilatational or transversal, and travel with their own velocity (c_t and c_d). Such velocity depends only on the material properties (for aluminum $c_d = 6100$ m/s and $c_t = 3100$ m/s.). For instance, the interference of a wave bouncing with an inclination of 45° gives the displacement field as shown in Fig. 4 [4]. If the bouncing wave is transversal, the resulting displacement pattern will be antisymmetric (A); if the bouncing wave is distortional, the displacement pattern will be symmetric (S).

In summary, the wave that propagates along the surface of a flat and infinite plate is the result of interference of waves traveling inside the material and the displacement pattern depends on the type and velocity of such constituent waves. There is a cut-off frequency for each Lamb wave, under which it cannot propagate. For plates with small thickness, only the first symmetric S_0 and antisymmetric A_0 Lamb waves are usually excited after a short time excitation (e.g. point impact). In the experimental results presented

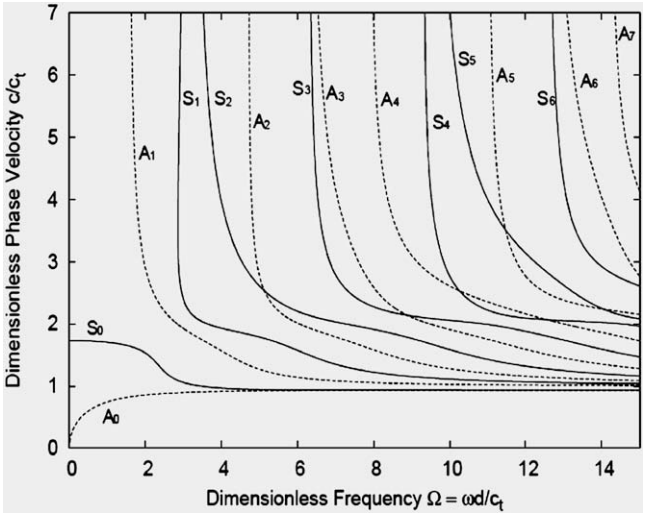

Fig. 2. Solutions of the wave equation for simple plates: dimensionless phase velocity as function of dimensionless frequency.

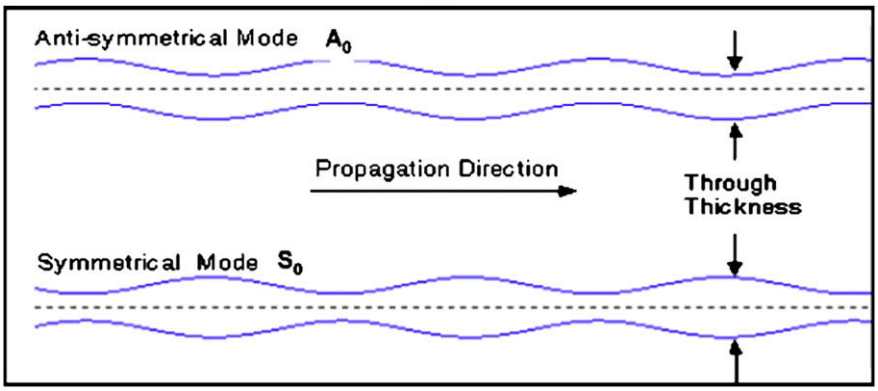

Fig. 3. Displacement pattern of A_0 and S_0 Lamb waves.

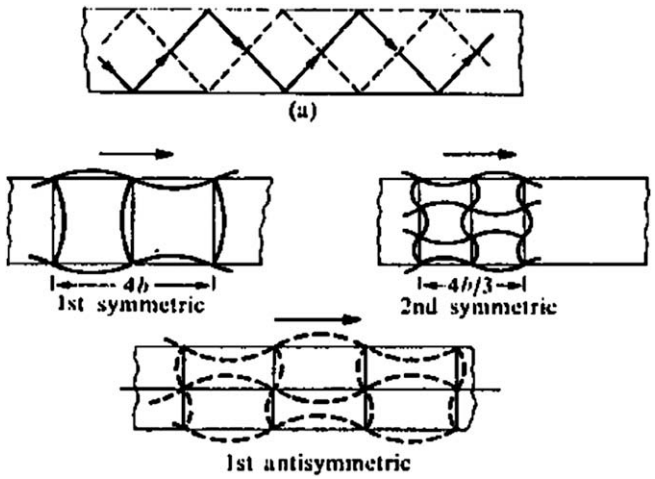

Fig. 4. The interference of waves bouncing at 45° inside the plate generates a Lamb wave (upper image). The mid image shows the resulting S_0 and S_1 symmetric modes, the lower image shows the A_0 mode.

hereafter, there will be only two excited wave modes. A real disturbance (wave group) results form interference of many Lamb waves with different frequencies, and in general Lamb waves experience dispersion. This means that their phase velocity depends on frequency. Therefore, a wave group can change its shape while propagating, since it may be composed by Lamb waves having different speeds of propagation.

Referring to Fig. 2, it appears that for dimensionless frequency below 2, the first symmetric S_0 Lamb wave is not dispersive, while the first antisymmetric A_0 is highly dispersive. Therefore, a wave group made by S_0 components will not change its shape while propagating, while a wave group made by A_0 components will grow wider in space, since its elementary components travel with different velocities. Therefore, the resulting wave group is dispersive. The velocity of the group (combination of elementary Lamb waves) is defined as:

$$c_g = c + k\frac{\partial c}{\partial k} \times \left(k = \frac{2\pi}{\xi}\right) \tag{3}$$

and equals the phase velocity of its components only if the wave is not a dispersive one (in this case $\partial c/\partial k = 0$ and the group wave speed is not a function of wavenumber or frequency).

3. Validation of the WT method

Before applying Wavelet analysis to waves generated by HVI, this method was validated in two steps. First, by perturbations generated by HVI on aluminum plate targets and simulated with a SPH code. Second, by acceleration signals generated by a low-velocity impact on a real Al plate and sampled with accelerometers. The objective was to identify by steps how the two wave modes (A_0

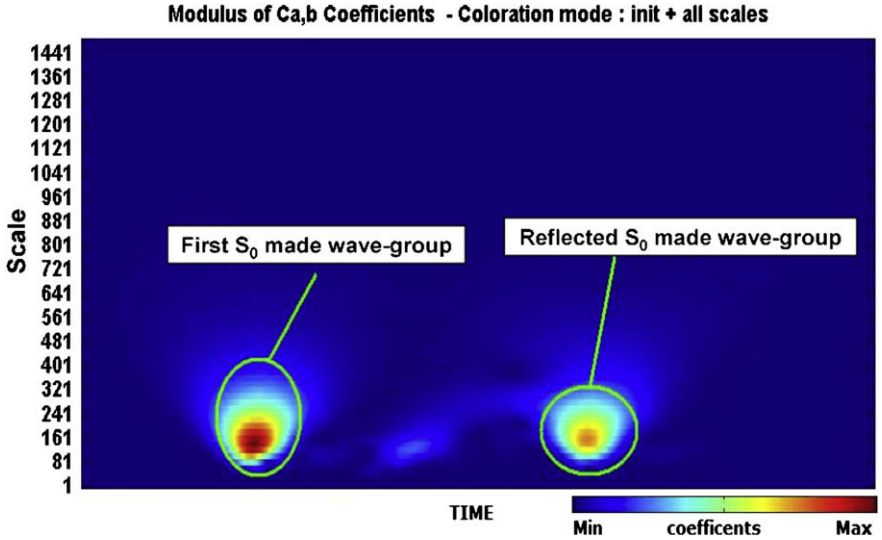

Fig. 5. WT spectrum of the S_0 made wave group.

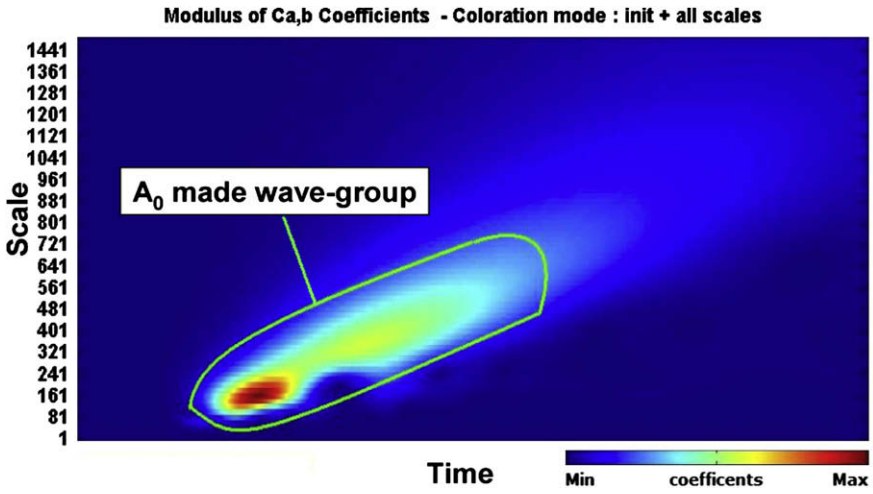

Fig. 6. WT spectrum of the A_0 made wave group.

and S_0) appear in a WT spectrum using signals of increasing complexity.

3.1. Numerical signals

A HVI simulation was performed with Autodyn 2D, on an Al-6061-T6 aluminum plate having size $300 \times 300 \times 0.8$ mm. Impact conditions referred to a 1 mm diameter Al-2084 sphere launched at 5 km/s. The total simulation time was 66 μs. The software allows for a separate calculation of the out of plane (OP) and in plane (IP) accelerations, which were acquired by a virtual sensor located in the mid plane of the plate 150 mm away from the impact point. Fig. 5 shows the resulting wavelet spectrum of IP waves. The plot presents in a color scale the magnitude of the WT coefficients, as a function of the time (horizontal axis) and the "scale", which is the inverse of the wave frequency (vertical axis). At any given frequency, the maxima of the WT represent the arrival time of each frequency component of the wave group.

Two bright spots are evident looking at Fig. 5, which represent wave groups made by S_0 Lamb waves. Since they appear in a WT spectrum like bright spots, the wave groups do not present a dispersive behavior. They have maintained an unchanged shape, because their frequency components (Lamb waves) travel with the same speed. The central frequency of the spots maxima (dark red in Fig. 5) is around 200 kHz. The maximum value of the left spot corresponds to the arrival of the first wave group at the virtual sensor, while that on the right represents the arrival time of the same wave, reflected from the plate boundaries. The group velocity of this weave is around 4.5 km/s. It has been computed simply from the ratio of the known distance between the sensor and the plate edge, and the time between the passage of the first and second spots in the WT spectrum. This velocity agrees very well with the theoretical value, in accordance with Fig. 2.

Similar considerations can be repeated for OP wave constituents (Fig. 6). In this case, only a stretched spot can be highlighted representing a wave in which high frequency components (low scale) arrive to the sensor in a shorter time with respect to low frequency ones (high scale). This means that high frequency constituents of OP group waves travel faster than low frequency ones. Referring again to Fig. 2, this represents a wave group made by A_0 Lamb waves, behaving like the one shown in Fig. 7. This wave group results form Lamb waves (A_0) which travel with different velocities. In this case, there is no evidence of the wave group made by S_0 Lamb waves because the virtual sensor is located on the plate mid plane. The displacement of S_0 Lamb waves is symmetric across the mid plane, so the resulting OP acceleration of this wave group is always zero (see Fig. 3).

3.2. Experimental signals – low-velocity impacts on simple plates

Impact tests were performed at both low velocity and hypervelocity. In particular, experiments were realized at the CISAS Impact Facility, using a Light Gas Gun, which is capable of accelerating 150 mg projectiles up to 5.8 km/s. Impact-induced accelerations were measured by Endevco 200k accelerometers (1.2 MHz resonance, 2×106 m/s^2 max acceleration peak) connected to amplifiers having bandwidth up to 400 kHz. The sampling frequency was of 5 MHz with a sampling window of 0.1 s. Test samples were aluminum (Al 2024-T81) $500 \times 500 \times 2$ mm plate, suspended by low stiffness springs inside the LGG vacuum chamber. In the case of low-velocity impacts, a steel ball with diameter equal to 5 mm was launched in a single-stage mode on a hanged Al thin plate. Fig. 8 (left) shows the sensor position and the impact point. Table 1 summarizes the accelerometer set-up. The aim of this test was to validate the wavelet method through the identification of wave modes using real signals. The sensors were directly fixed to the plate surface. In this case, only OP acceleration can be sampled (both the S_0 and A_0 made wave group have OP acceleration components).

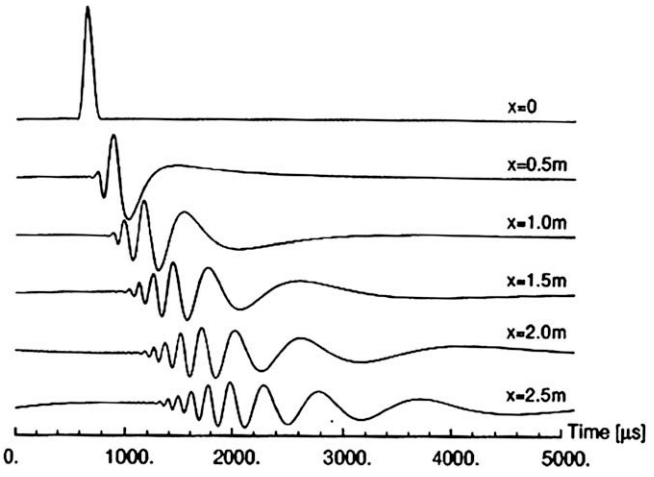

Fig. 7. Example of a dispersive wave: it changes its shape while propagating. This occurs because the phase velocity of its constituents is different. In this case, constituents with high frequency travel faster than low frequency ones.

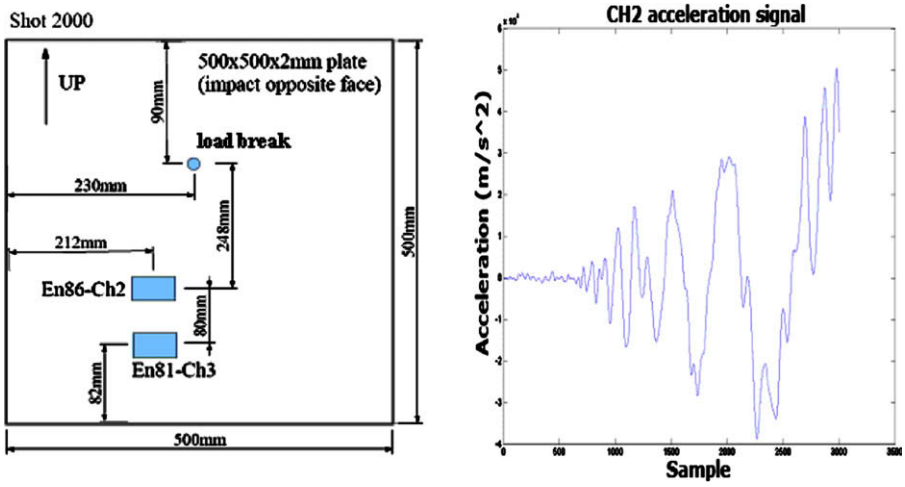

Fig. 8. On the left is shown low-velocity impact set-up, on the right, the earlier part of the Ch2 acceleration signal.

Table 1
Summary of the accelerometers used in low-velocity impact on thin aluminum plate

Sensor	Accelerometer range (m/s^2)	Distance from the impact point (mm)	Channel	Plate fixing method
Endevco 200k	2×10^6	248	Ch2	Acrylic glue
Endevco 200k	2×10^6	328	Ch3	Acrylic glue

Fig. 9 shows the WT spectrum of the Ch2 signal. The *x*-axis reports the time shift, while the *y*-axis is the scale (inverse of the frequency). The high frequency part of the perturbation travels faster than the low frequency one; in fact, the red part of the spectrum (high value of the coefficients) appears first for low values of the scale (high frequency). This feature highlights that this wave group (dispersive) is made by A_0 Lamb waves. The phase velocity of the wave group components follows the dispersion characteristics reported in Fig. 2. The arrival time of each wave constituent may be evaluated from horizontal sections of the plot of Fig. 9. Fig. 10 shows the time variation of the WT coefficients at 30 kHz frequency: the Lamb wave arrives at the sensor at time $\cong 15$ ms. We can repeat this evaluation for the other wave components (with different frequencies), thus obtaining the arrival time for each of them. Referring to the second sensor (Ch3), the dispersion feature can be computed in a similar way.

The phase speed of each component is derived using the following formula:

$$c_{\mathrm{ph}}(f) = \frac{y_2 - y_1}{b_2(f) - b_1(f)} \tag{4}$$

where C_{ph} is the velocity of each Lamb wave, $y_2 - y_1$ is the distance between the sensors and $b(f)$ is arrival time of each wave (this is identified by the peak maxima for each constant-frequency line in the WT spectra). Table 2 summarizes the phase velocities computed for each frequency.

Fig. 11 shows the phase speed for the Lamb waves computed with the above method. The curve shown is fully compatible with the A_0 Lamb waves at the same frequency range (see Fig. 2). Moreover, since the low-velocity impact is not perforating, the S_0 made wave group has not been excited. In fact, no spots appear in the WT spectrum.

4. HVI on simple aluminum plates

In previous chapters, the WT method was explored through its application to numerical (SPH) and simplified experimental test

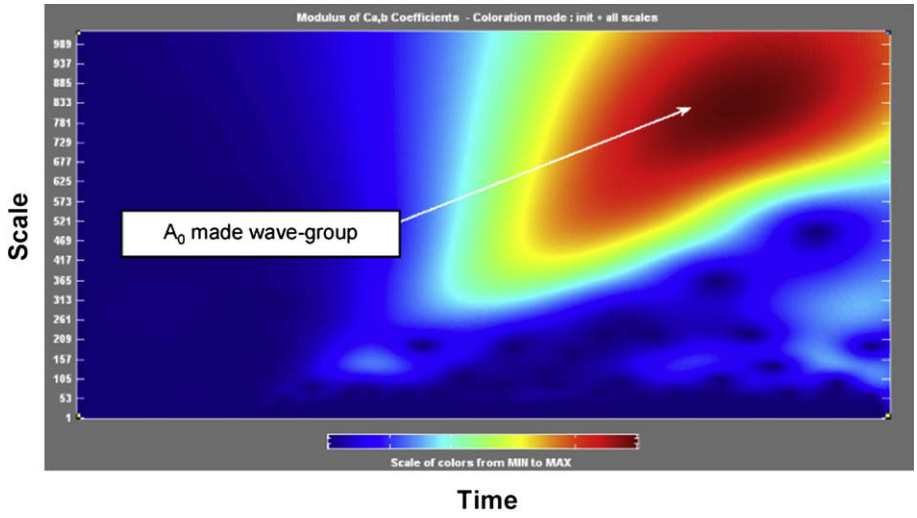

Fig. 9. WT spectrum of the Ch2 acceleration signal.

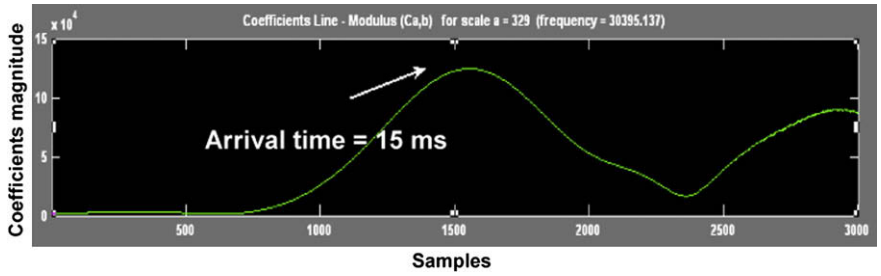

Fig. 10. Section of the WT spectrum at 30 kHz and scale 329.

Table 2
Phase velocities of the A_0 made wave group

Frequency (kHz)	Scale	Phase velocity (m/s)
30	329	1900 ± 250
25	391	1500 ± 250
21	464	1200 ± 250
14	694	1000 ± 250

cases. At this point, a qualitative analysis of the disturbance field produced by HVI on simple plates and honeycomb panels is presented, using the methods above mentioned. This section deals with HVI on simple aluminum plates; Section 5 reports on HVI tests on honeycomb aluminum panels. The target plate was hanged inside the LGG vacuum chamber. A 1.5 mm diameter projectile was launched at 4700 m/s. The target set-up is shown in Fig. 12. Hypervelocity impacts on thin plates generate signals with very high amplitude and frequency content. This requested to place sensors far away form the impact points. They were attached using adhesive tape instead of acrylic glue, to ease the accelerometers detachment after tests. The adhesive tape was experimentally validated and it does not interfere with the acceleration measurement.

The lower scale peaks of the WT coefficients (as shown in Fig. 13) correspond to a frequency of 166 kHz. Since there is no dispersion, each peak represents the arrival time of a S_0 made wave group.

Fig. 14 shows the constant scale plot (scale 6 in Fig. 13). Computing the time shift between the first peak (at 166 kHz) of Ch1 WT spectrum and the fist peak at the same frequency of the Ch3 WT spectrum, the wave group speed results 5380 ± 250 m/s. In fact, for a not dispersive wave the phase speed coincides with the group speed. This is in good accordance with the group wave speed predicted analytically for the same perturbation propagating in a 2 mm thickness plate and having a frequency of 166 kHz. The peaks following the first one represent reflections of the wave at the plate boundaries.

Comparing the group speed to that of the first case presented (SPH simulation), this wave group seems to travel faster. This is due to the lower frequency of its components. The central frequency of the wave group in the SPH simulation was 200 kHz and it experiences dispersion, because it is made by high frequency Lamb waves. Instead, the group wave generated by the HVI has a lower central frequency of 166 kHz and thus experiences less dispersion. For this reason, the group velocity of this wave is higher (remember the velocity/frequency relation of Eq. (3)).

The wide spot at scale between 24 and 64 (corresponding to 41 kHz and 16 kHz, respectively) represents an A_0 made wave group. In fact, it shows a strong dispersion behavior, as seen for the low-velocity impact (Fig. 7). The ratio between the Ch1 and Ch3 distance and the time shift between the arrival time of their first peak in the WT spectrum (at 20 kHz), gives a wave phase speed of 1100 ± 250 m/s. This computation can be made for various frequency values (like in the low velocity test), and the results are again in good accordance with the analytical solution shown in Fig. 2.

5. HVI on honeycomb aluminum panels

HVI tests were performed on all-aluminum honeycombs sandwich panels, having size $400 \times 400 \times 52.7$ mm and skin thickness

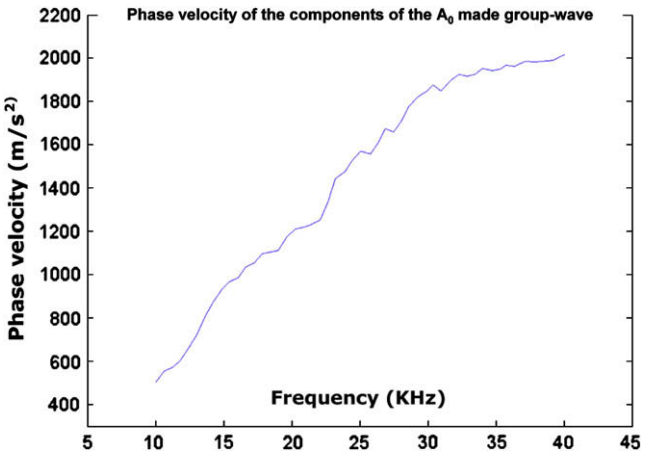

Fig. 11. Dispersion feature for the components of the A_0 made wave group.

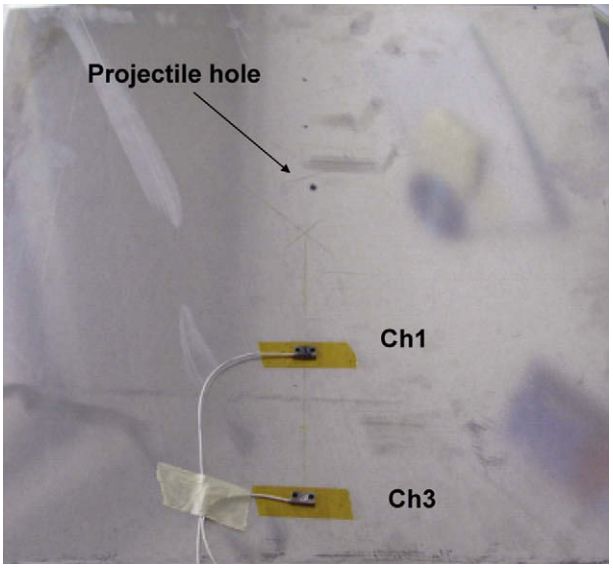

Fig. 12. Target set-up with accelerometers.

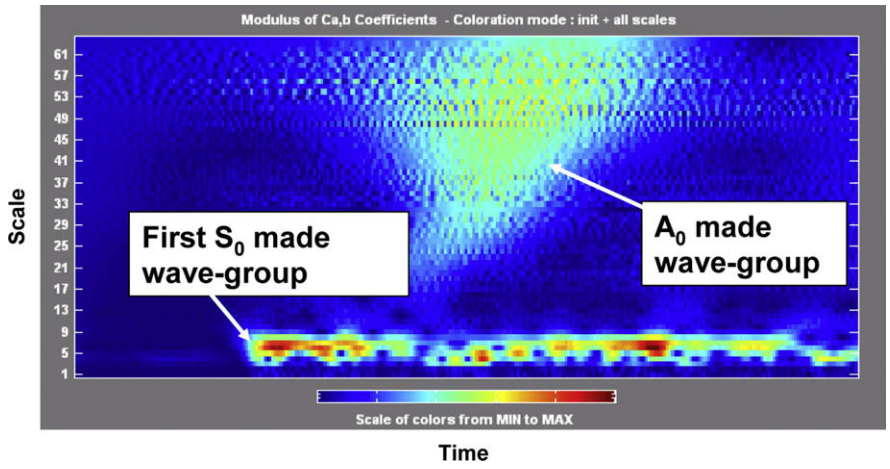

Fig. 13. The WT spectrum of the signal as recorded by Ch1.

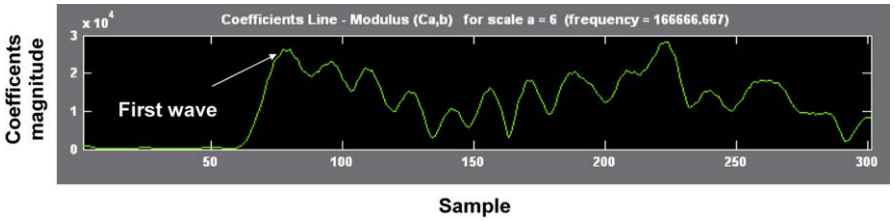

Fig. 14. WT spectrum of Ch1 at constant scale value, corresponding to 166 kHz.

equal to 1 mm. Projectiles were 2.3 mm diameter aluminum spheres launched at 5 km/s. Such impact conditions resulted in the target complete perforation. Impact-induced accelerations were measured by four Endevco 200k accelerometers connected to amplifiers having bandwidth up to 400 kHz. The sampling frequency was 5 MHz with a sampling window of 0.1 s. In the following, the description of the results of the most representative experiment is presented. Fig. 15 shows the test target and the accelerometers set-up. The Endevco sensors were connected directly on the impacted honeycomb skin, with adhesive tape. Table 3 shows the accelerometers used on this test.

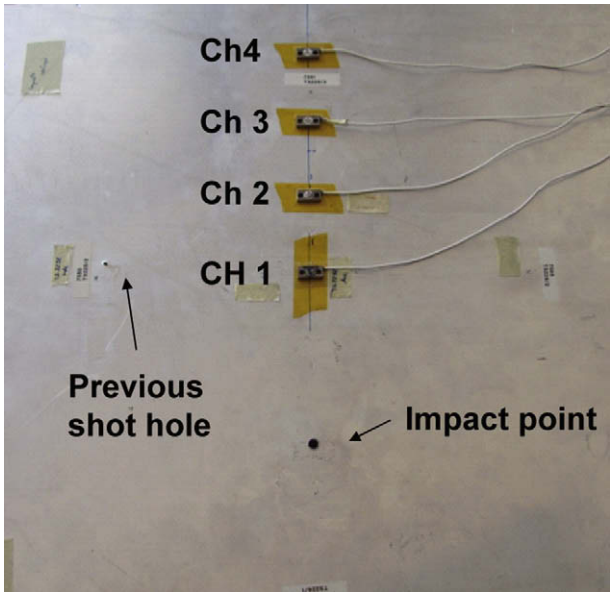

Fig. 15. Honeycomb test target: four accelerometers were attached on the panel aluminum skin (on the left is visible a small hole, resulting from a past impact).

The WT spectrum computed on the acceleration signal recorded by sensor number 1 (Ch1) is shown in Fig. 16. The first peak in the WT spectrum represents the arrival of the first wave group. The group central frequency is 160 kHz, the same in all spectra. Since there is no evidence of dispersion, this wave group is made only by S_0 waves. Its group velocity can be computed comparing the arrival times at each sensor couple. The three computed velocities are shown in Table 4.

Looking at the four WT spectra there is no evidence of a wave group made by A_0 Lamb waves. This is probably due to the high flexural stiffness of the honeycomb plate. Instead, in all spectra there are many other peaks after the first one. Fig. 17 shows the coefficient line at 160 kHz of the wavelet spectrum for sensor 1.

In the following text, the velocity measurements' uncertainty is always ± 250 m/s. The second peak is smaller and wider with respect to the first. It coincides with a wave traveling at 5200 m/s and reflected back by the second accelerometer. The third peak corresponds to a wave reflected from a pre-existing hole in the plate (a past HVI impact). Its propagating velocity of 5200 m/s demonstrates this.

Table 3
Summary of the accelerometers used for hypervelocity impact on honeycomb panels

Sensor	Accelerometer range (m/s^2)	Distance from the impact point (mm)	Channel	Plate fixing method
Endevco 200k	2×10^6	100	Ch1	Adhesive tape
Endevco 200k	2×10^6	150	Ch2	Adhesive tape
Endevco 200k	2×10^6	200	Ch3	Adhesive tape
Endevco 200k	2×10^6	250	Ch4	Adhesive tape

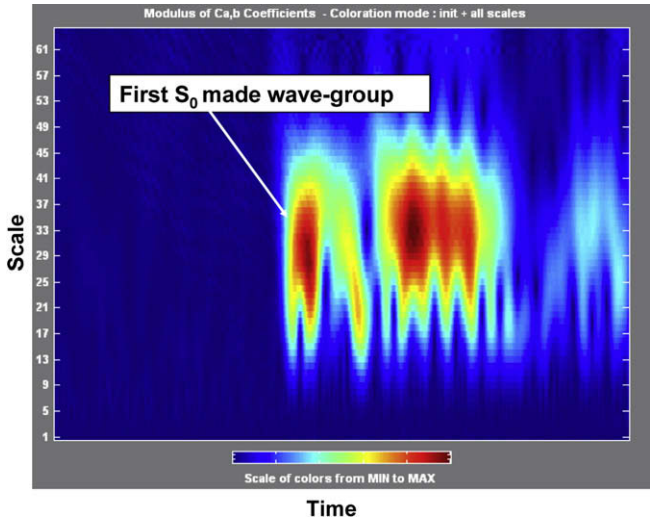

Fig. 16. Wavelet spectrum of the acceleration signal recorded by sensor number 1 (scale = 30 corresponding to 160 kHz frequency).

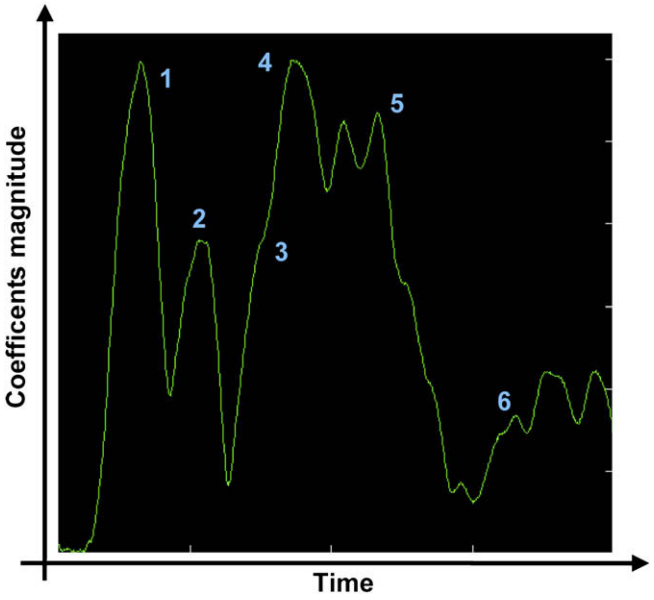

Fig. 17. Section of the WT spectrum of Fig. 16, corresponding to 160 kHz frequency (scale = 30).

Table 4
Speed of propagation of the first wave group, computed though the comparison of waves arrival times between each sensor couple

Sensor 1–2 (m/s)	Sensor 2–3 (m/s)	Sensor 3–4 (m/s)
5102 ± 250	5400 ± 250	5208 ± 250

Peak number 4 coincides with the wave propagated on the back honeycomb plate, and transmitted to the sensor through the lamina of the honeycomb core connecting the two A_l skins. The projectile was supposed to travel through the honeycomb thickness with its impact velocity of 4950 m/s, while the wave transmitted by the core's lamina was supposed to be an A_0 made wave traveling at 1600 m/s. This last velocity value is confirmed by peak number 7, which coincides exactly with the arrival time of the same wave, bouncing between the front and the back A_l plates. Peak number 5 represents the arrival time of the wave reflected by the lateral edges of the plate (traveling at 5200 m/s) and also the arrival time of the wave reflected by the impact hole (traveling at 5200 m/s). Peak number 6 corresponds to the wave reflected from the most distant edge, located behind sensor number 4 and traveling at 5130 m/s.

This analysis was made for the other three spectra with the same results. Every wave reflected or scattered coincides to a feature in the WT spectra: a peak or an inflection point. The wave behavior becomes rapidly complex after some reflections, and it is very hard to identify them all. However, this has demonstrated that the WT can successfully identify waves propagating in honeycomb panels after HVI.

6. Conclusions

This paper presented the application of the Wavelet Transform (WT) analysis to study the transient waves propagating in plates and honeycomb sandwich panels as a consequence of impacts at hypervelocity. Two types of wave groups have been experimentally observed on simple plate target. The first group is made by symmetric (S_0) Lamb waves, while the second by antisymmetric (A_0) (symmetry and antisymmetric respect to the plate's mid plane). Wavelet analysis was able to identify both the frequency content and the propagation velocity. In case of the non-perforating impact, antisymmetric group waves are predominant (see low velocity test). On honeycomb-panel-skins the symmetric waves are dominant. Antisymmetric waves have not been identified, probably due to the high stiffness of the plate (which determines flexural A_0 Lamb waves with very low amplitude). Moreover, on honeycomb panel, reflections on edges and discontinuity have been captured. As a summary, the use of the Wavelet Transform for the analysis of acceleration data demonstrated the possibility of identifying perturbations propagating after an impact. Special applications are the detection of the wave's constituents and the separation of the original wave from its reflections. This makes it possible to generalize experimental results obtained on laboratory-scaled targets on which edge effects may play an important role.

References

[1] NASA Technical Standard Pyroshock test criteria, NASA-STD-7003; 1999.
[2] Graff KF. Wave propagation in elastic solids. Oxford: Calderon Press; 1975.
[3] Meo M, Zumpano G. Impact identification on a sandwich plate from wave propagation responses. Composite Structures 2005;71:302–6.
[4] Wang L, Yuan FG. Group velocity and characteristic wave curves of Lamb waves in composites: Modeling and experiments. Composites Science and Technology 2007;67:1370–80.
[5] Park HC, Kim DS. Evaluation of the dispersive phase and group velocities using harmonic wavelet transform. NDT and E International 2001;34:457–67.
[6] Newland DE. Harmonic wavelets in vibrations and acoustics. Philosophical Transactions of the Royal Society of London, Series A 1999;357:2607–25.